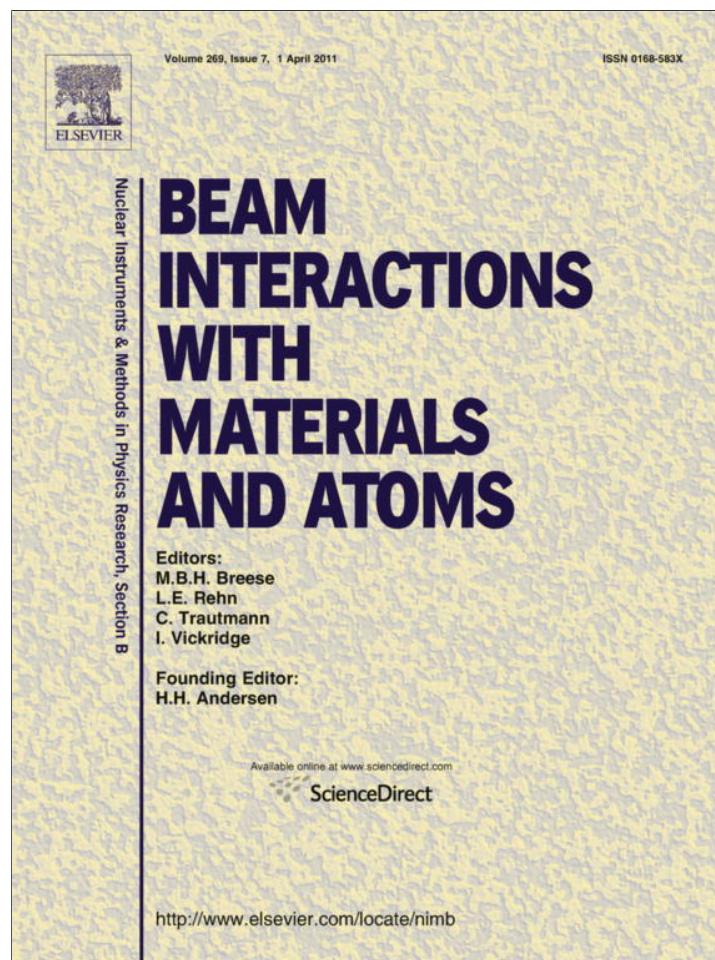


Provided for non-commercial research and education use.  
Not for reproduction, distribution or commercial use.



This article appeared in a journal published by Elsevier. The attached copy is furnished to the author for internal non-commercial research and education use, including for instruction at the authors institution and sharing with colleagues.

Other uses, including reproduction and distribution, or selling or licensing copies, or posting to personal, institutional or third party websites are prohibited.

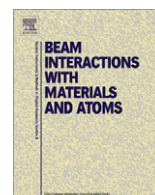
In most cases authors are permitted to post their version of the article (e.g. in Word or Tex form) to their personal website or institutional repository. Authors requiring further information regarding Elsevier's archiving and manuscript policies are encouraged to visit:

<http://www.elsevier.com/copyright>



Contents lists available at ScienceDirect

## Nuclear Instruments and Methods in Physics Research B

journal homepage: [www.elsevier.com/locate/nimb](http://www.elsevier.com/locate/nimb)

## Precision and accuracy of two luminescence dating techniques for retrospective dosimetry: SAR-OSL and SAR-ITL

Vasilis Pagonis\*, Atlee Baker, Meredith Larsen, Zachary Thompson

Physics Department, McDaniel College, Westminster, MD 21157, USA

### ARTICLE INFO

#### Article history:

Received 28 September 2010  
Received in revised form 5 October 2010  
Available online 1 February 2011

#### Keywords:

Thermoluminescence  
TL  
Isothermal-TL  
Optically stimulated luminescence  
OSL  
Equivalent dose estimation  
Quartz  
Retrospective dosimetry  
Authenticity testing  
Accident dosimetry  
Kinetic rate equations  
SAR technique

### ABSTRACT

Luminescence techniques based on thermally or optically stimulated signals are used extensively for estimating the equivalent dose (ED) of quartz samples for dating and retrospective dosimetry. This paper presents simulations of two luminescence dating protocols which use single aliquots of the quartz samples. The first protocol is the well-known single-aliquot regenerative optically stimulated luminescence (SAR-OSL) protocol for quartz. The second protocol was developed more recently and is based on a thermoluminescence (TL) signal measured under isothermal conditions (termed the SAR-ITL technique). The simulations are carried out using a recently published comprehensive kinetic model for quartz, consisting of 11 electron and hole traps and centers. The complete sequence of the two experimental protocols is simulated using the same set of kinetic parameters. The simulated dose response curves for the two protocols are found to be very similar to published experimental data. The relative intrinsic accuracy and precision of the two techniques is estimated by simulating one hundred random variants of the natural samples, and by calculating the equivalent doses using each technique. The 100 simulated natural variants are generated by keeping the transition probabilities between energy levels fixed, while allowing simultaneous random variations of the concentrations of the 11 energy levels. The SAR-OSL protocol was found to be intrinsically both more accurate and more precise than the SAR-ITL protocol. We investigate several experimental factors which affect the precision and accuracy of the two protocols. New simulations are presented for commonly used sensitivity tests consisting of successive cycles of sample irradiation with the same dose, followed by measurements of the sensitivity corrected  $L/T$  signals. These new simulations provide valuable insight into the previously reported sensitivity changes taking place during application of the SAR-ITL protocol.

© 2011 Elsevier B.V. All rights reserved.

### 1. Introduction

Luminescence techniques are well-established experimental methods for determining the total cumulative dose from natural radiation sources, for accident dosimetry and for archaeological authenticity testing [5,9,10,34,33]; and references therein). During the past 4 decades accurate and precise methods have been developed for estimating the equivalent dose (ED) in samples containing quartz; such methods are based either on thermoluminescence (TL) signals, or more recently on optically stimulated luminescence (OSL) signals. In a recent comprehensive review of luminescence dating techniques Wintle [33] summarized the historical and technological developments in luminescence dating during the past 50 years.

Although TL and OSL dating techniques are well established experimentally, further theoretical and modeling work is needed in order to obtain a better understanding of the various factors

influencing both the precision and the accuracy of the experimental protocols. There have been several published experimental and simulation attempts to estimate the precision and accuracy of various TL/OSL dating techniques.

This paper describes an effort to simulate the complete experimental protocols for two very different luminescence dating techniques, and to estimate their relative intrinsic accuracy and precisions. The first technique is the well-known SAR-OSL technique (single-aliquot regenerative dose optically stimulated luminescence) and is based on optically stimulated luminescence signals; this is a well established technique that has been applied successfully to numerous quartz samples over the past 10 years [34]. There have been several notable published attempts to simulate the SAR-OSL technique and to obtain an estimate of its accuracy and precision, and these are summarized in the next section.

The second luminescence dating technique was developed much more recently and is based on TL signals measured under isothermal conditions. In the rest of this paper we will refer to this latter technique as the SAR-ITL technique (single-aliquot regenerative isothermal-TL technique). While there have been several

\* Corresponding author. Tel.: +1 410 857 2481; fax: +1 410 386 4624.

E-mail address: [vpagonis@mcDaniel.edu](mailto:vpagonis@mcDaniel.edu) (V. Pagonis).

published simulations of the SAR-OSL technique, there are no published simulations of the SAR-ITL technique in the literature, and this paper presents such a first attempt. Previous experimental work on the SAR-ITL protocol is summarized in a subsequent section.

The purpose of this paper is to simulate the intrinsic accuracy and precision of these two different techniques by using a statistical ensemble approach. The statistical variation of the intrinsic accuracy and precision of the two techniques is estimated by simulating random variations of the concentrations of electrons and holes in natural quartz samples, using a recently published comprehensive model for quartz [25]. The SAR-OSL protocol was found to be more accurate than the isothermal-TL technique, but its dose range is more limited. The simulated average dose response curves for the two techniques are similar to published experimental data. The paper presents new simulations of sensitivity changes occurring during the two protocols, and these simulated results provide useful insights into the experimentally reported inaccuracies of the SAR-ITL protocol for some quartz samples.

## 2. Previous modeling work on the SAR-OSL protocol

There have also been several notable published experimental and simulation attempts to estimate the precision and accuracy of various TL/OSL dating techniques [1,2,6–8,22,24–26]. McKeever et al. [22] carried out simulations using a simple OSL model in order to examine the assumptions behind the SARA dating technique. Their simulations showed that the extent of bleaching of the OSL signal and the laboratory/natural doses are a significant source of sensitivity changes. However, they concluded that these sensitivity changes depend only weakly on the added doses, and hence these should not affect the SARA protocols significantly.

Chen et al. [15] provided a simple model of the SAR-OSL procedure, in which they assumed that two electron traps gave rise to the OSL signal  $L$ . This signal was represented mathematically in the model by a two-component saturating exponential. Furthermore, it was assumed that the probability of trapping electrons in this system does not change with repeated use of the phosphor, and that the two-saturating exponentials equation applies to all OSL measurements made after all sample irradiations carried out with the same aliquot. These authors also expressed mathematically the intensity of the test dose signal  $T$ , and hence obtained an expression for the sensitivity-corrected dose–response curve ( $L/T$ ) plotted against the regenerative dose  $D$ . This expression was fitted using four independent parameters, and the simulation results agreed with experimentally measured dose responses.

Bailey [7] used a Monte Carlo approach in which a “standard” quartz model was used as a starting point and 300 versions of the parameters were generated by randomly selecting concentration values within  $\pm 80\%$  of the original values, by using uniformly distributed random numbers. For each of these variants the full sequence of irradiation and thermal history of the samples were simulated, and the SAR-OSL protocol was simulated in order to obtain an estimate of its accuracy and precision. Bailey [7] studied the effect of several experimental factors on the accuracy of the SAR-OSL technique, including the preheat temperature and irradiation temperature of the sample. He found that the simulated SAR-OSL technique overestimated systematically the ED of the sample, and suggested the use of pulsed irradiation as a possible method of correcting for these overestimates.

Pagonis and Carty [23] used a modified version of the model by Chen and Leung [13,14] to simulate the complete sequence of experimental steps taken during the additive dose version of the predose technique. Their simulation results showed that the

additive dose technique can reproduce accurately the accumulated dose or paleodose (PD) received by the sample with an accuracy of  $\pm 1\text{--}5\%$  over several orders of magnitude of the paleodose. This simulation study was expanded by Pagonis et al. [25] using the comprehensive model by Bailey [6]. These authors simulated both the additive dose and the multiple activation versions of the predose technique, as well as the very successful single-aliquot regenerative optically stimulated luminescence (SAR-OSL) protocol. The results of these simulations showed that the SAR-OSL protocol is in general less sensitive to the specific experimental conditions, than either the additive dose or the multiple activation techniques.

Duller [17] discussed the nature of random and systematic sources of error in measurements of the equivalent dose ED during SAR-OSL measurements. He identified as possible sources of systematic errors the following: errors in calibration of beta or gamma sources used for sample irradiation, as well as uncertainties due to the suitability of the materials used during the SAR protocol. He examined several approaches to estimating the error in ED in the linear dose response region of the OSL signal. The errors in individual sensitivity corrected luminescence signals ( $L/T$  ratios) were estimated using the uncertainty due to counting statistics, as well as what was collectively termed “instrumental error”. The latter includes such sources of experimental uncertainty as variation in the intensity of the irradiator and optically stimulating source, aliquot positioning under the source and temperature variations during the  $L$  and  $T$  signals. Duller [17] used an overall estimated value of 1% to describe the instrumental error. By performing an error analysis of these various factors, estimates of the combined error in ED were obtained. Duller also used an alternative approach based on a more robust Monte Carlo method of analysis. In this method of analysis each value of the sensitivity corrected OSL signal  $R_x$  and its corresponding error  $S_{R_x}$  is represented by a Gaussian distribution of possible values (with the error  $S_{R_x}$  based on counting statistics and instrumental error). Repeated curve fitting and calculations of ED are carried out by using values of  $R_x$  from the Gaussian distribution whose widths are set by the calculated standard deviations. The resulting distributions of ED values are then analyzed to estimate the error in ED. Duller [17] found that these two very different approaches gave consistent results which were very close to each other.

A different approach was used by Rhodes [27], in which a probabilistic numerical model was used to construct synthetic ED distributions. Simulated OSL from grains of different sensitivities and with various simulated ED values were combined, resulting in complex simulated patterns. Several examples of experimental single grain OSL sensitivity distributions were presented, providing demonstrations of the effects resulting from natural differences. The minimum age model was used to analyze synthetic ED values.

Thompson [28] performed Monte Carlo simulations of SAR OSL dosimetry measurements to investigate the behavior of the measured equivalent dose as a function of absorbed dose (also termed the burial dose). It was found that the mean ED value overestimated the palaeodose, particularly for larger luminescence measurement errors and for larger paleodoses. These simulations showed that the median ED value was a more accurate estimate of the palaeodose at moderate paleodoses. In addition, it was found that exponential dose sequences yield similar accuracy and precision as linear dose sequences, while reducing the total irradiation time. A minimal dose sequence was proposed and was shown to require even less total irradiation per sample than exponential dose sequences, while maintaining accuracy (within 1%) and precision (standard deviation of 1–6%) for 24 aliquots measured with a reasonable luminescence measurement error of 2%. The results of these simulations showed that significant savings in total irradiation time per sample are possible.

### 3. Previous experimental work on the SAR-ITL protocol

Several researchers studied the ITL signal at 310 °C and found it continues to grow to much higher doses than the optically stimulated luminescence (OSL) signal [20,21,16]. These earlier studies concluded that this ITL signal which seems to originate at the 325 °C region of the TL glow curve, is thermally stable and can be fully reset by sunlight. Subsequent research found that the ITL signal at 310 °C can be used successfully with a single-aliquot regenerative-dose protocol, and this was termed the SAR-ITL protocol. This protocol was applied successfully to several quartz samples [20,16]. However, later work on other sedimentary samples showed that the SAR-ITL protocol based on the quartz ITL signal at 310 °C overestimates the expected equivalent dose [12,19]. This overestimation is believed to be caused by an irreversible sensitivity change that occurs at some stage during measurement of the natural ITL signal, and may preclude the reliable use of the SAR-ITL protocols.

Vandenberghé et al. [29] recently reported on the use of an isothermal thermoluminescence (ITL) signal for determining the equivalent dose ED in unheated sedimentary quartz. In order to minimize the above mentioned sensitivity change during the first measurement, the ITL signal was measured at 270 °C following a preheat for 10 s at 300 °C. Furthermore, it was found that this ITL signal grows with dose over at least the same range as the OSL signal. This recent study provided several examples for the large variability in the ITL dose response of different quartz samples. For some samples the ITL signal measured at 270 °C exhibited the exact same growth characteristic as the OSL signal, while in other samples this signal continued to grow to higher doses. It was concluded that in the latter cases the ITL signal has the potential to extend the age range, especially for quartz samples where the OSL signal saturates below 500 Gy.

Vandenberghé et al. [29] found that a single-aliquot regenerative-dose (SAR-ITL) protocol could be used with this ITL signal, and dose recovery experiments were carried out successfully. Several dose recovery tests were carried out by adding a known laboratory dose on top of the natural dose in recently deposited samples. These samples were then measured using the SAR-ITL protocol. The authors explicitly avoided artificially reset samples, because previous work suggested that laboratory bleaching might adversely affect the sample properties [19]. It was concluded that both laboratory and natural doses can be accurately determined using a SAR-ITL protocol based on the ITL signal measured at 270 °C, following a preheat of 10 s at 300 °C. There was no evidence for significant desensitization during the first measurement in this study. This is in contrast to previous studies that used the ITL signal at 310 °C, which reported a large overestimation of both given and natural doses [12,19].

### 4. Description of the model

The simulations in this paper are carried out using the comprehensive quartz model developed by Pagonis et al. [25]. This model is based on a previous model by Bailey [6] that was developed on the basis of empirical data. Fig. 1 shows the energy level diagram for the model used in this paper. The set of differential equations and the choice of parameters were presented recently by Pagonis et al. [25], and will not be repeated here. For easy reference we briefly describe here the various energy levels in the model, as well as present the values of the kinetic parameters in Table 1.

The original model by Bailey [6] consists of five electron traps and four hole centers, and has been used successfully to simulate a wide variety of TL and OSL phenomena in quartz. This model was expanded by Pagonis et al. [25] to include two additional lev-

els (10 and 11 in Fig. 1), as described below. Level 1 in the model represents a shallow electron trapping level, which gives rise to a TL peak at ~100 °C with a heating rate of 5 K/s. The TL and OSL signal from this trap do not play a major role in the simulations of this paper. Level 2 represents a generic “230 °C TL” trap, typically found in many quartz samples. The TL signal from this trap has been used successfully in several comprehensive dating studies [11,18].

Levels 3 and 4 are usually termed the fast and medium OSL components and they yield TL peaks at ~330 °C as well as giving rise to OSL signals. The OSL from levels 3 and 4 forms the basis of the very precise and accurate SAR protocols [34]. The model does not contain any of the slow OSL components which are known to be present in quartz, and which were incorporated in later versions of the model [7]. Level 5 is a deep electron center which is considered thermally disconnected. Levels 6 and 7 are thermally unstable, non-radiative recombination centers (also known as “hole reservoirs”). These two levels play a crucial role in the predose sensitization mechanism which forms the basis of the predose dating technique [26].

Level 8 is a thermally stable, radiative recombination center often termed the “luminescence center” (L). Level 9 is a thermally stable, non-radiative recombination center termed a “killer” center (K). Levels 10 and 11 are the two new levels added to the original Bailey model by Pagonis et al. [25], and were introduced in order to simulate the experimentally observed thermally transferred OSL (TT-OSL) signals and basic transferred OSL (BT-OSL) signals [30–32]. Level 10 in the model represents the source trap for the TT-OSL signal and is a slightly less thermally stable trap with high dose saturation. It is assumed that electrons can be thermally transferred into the fast component trap (level 3) from level 10 by a single transfer mechanism [3,4,25]. This trap (level 10) is assumed to be emptied optically in nature by long sunlight exposure. Level 11 is believed to contribute most of the BT-OSL signal in quartz; they are believed to be light insensitive traps which are more thermally stable than either level 3 or level 10.

The kinetic parameters in Table 1 are as defined by Bailey [6];  $N_i$  are the concentrations of electron traps or hole centers ( $\text{cm}^{-3}$ ),  $n_i$  are the concentrations of trapped electrons or holes ( $\text{cm}^{-3}$ ),  $s_i$  are the frequency factors ( $\text{s}^{-1}$ ),  $E_i$  are the electron trap depths below the conduction band or hole trap depths above the valence band (eV),  $A_i$  ( $i = 1-5$ , and  $i = 10,11$ ) are the conduction band to electron trap transition probability coefficients ( $\text{cm}^3 \text{s}^{-1}$ ),  $A_j$  ( $j = 6-9$ ) are the valence band to hole trap transition probability coefficient ( $\text{cm}^3 \text{s}^{-1}$ ), valence band to trap transition probability coefficients ( $\text{cm}^3 \text{s}^{-1}$ ) and  $B_j$  ( $j = 6-9$ ) are the conduction band to hole center transition probability coefficients ( $\text{cm}^3 \text{s}^{-1}$ ). Other parameters related to the photoionization cross-sections of the optically sensitive traps are the photo-ejection constant  $\theta_{0i}$  ( $\text{s}^{-1}$ ) at  $T = \infty$ , the thermal assistance energy  $E_i^{\text{th}}$  (eV). The numerical values given in Table 1 are those given in Table 2 of Pagonis et al. [25].

In all simulations presented in this paper we simulate the irradiation of quartz samples in nature as realistically as possible, by assuming that the quartz sample has received burial doses with a natural dose rate of  $3 \times 10^{-11}$  Gy/s. By contrast, laboratory simulations are simulated at a much higher dose rate of 1 Gy/s.

In the rest of this paper it will be demonstrated that using the set of parameters in Table 1, it is possible to simulate the complete experimental protocols for the SAR-OSL and SAR-ITL dating protocols. Tables 2 and 3 show in schematic form the simulation steps for obtaining the dose response curves for the SAR-OSL and SAR-ITL dating techniques respectively. Tables 4 and 5 show in schematic form the simulation steps in a typical application of the two protocols, in order to obtain the equivalent dose of the quartz samples.

There are some additional relaxation steps in the simulations which are not shown explicitly in Tables 2–5. Specifically after

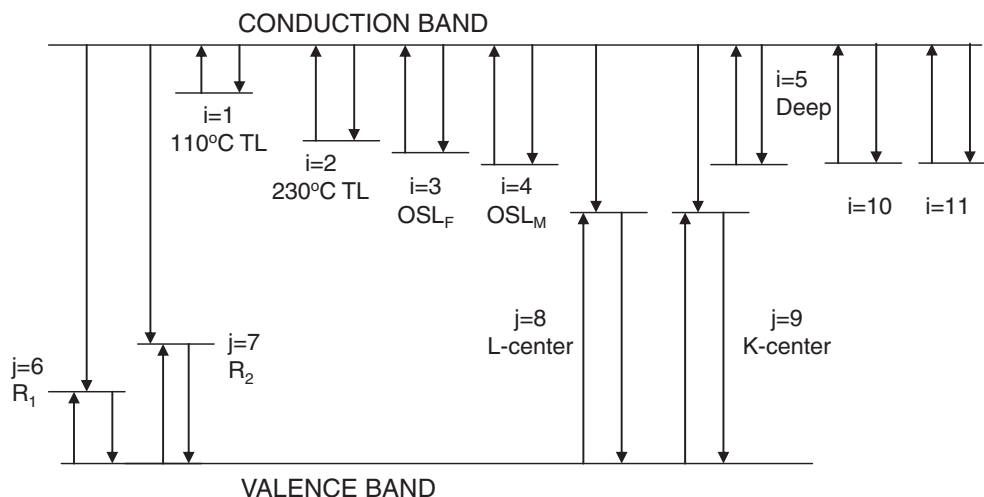


Fig. 1. Schematic diagram of the comprehensive quartz model of Pagonis et al. [25] used in this paper. The kinetic parameters used in this model are given in Table 1.

**Table 1**  
The parameters of Pagonis et al. [25] are shown together with modified values for  $N_{10}$  and  $N_{11}$  introduced in the present simulations shown in bold.

	$N_i$ cm <sup>-3</sup>	$E_i$ eV	$s_i$ s <sup>-1</sup>	$A_i$ cm <sup>3</sup> s <sup>-1</sup>	$B_i$	$\theta_{0i}$ s <sup>-1</sup>	$E_i^{th}$ eV
1	1.5e7	0.97	5e12	1e-8		0.75	0.1
2	1e7	1.55	5e14	1e-8		0	0
3	4e7	1.73	6.5e13	5e-9		6	0.1
4	2.5e8	1.8	1.5e13	5e-10		4.5	.13
5	5e10	2	1e10	1e-10		0	0
6	3e8	1.43	5e13	5e-7	5e-9	0	0
7	1e10	1.75	5e14	1e-9	5e-10	0	0
8	3e10	5	1e13	1e-10	1e-10	0	0
9	1.2e12	5	1e13	1e-14	3e-10	0	0
10	5e9	1.65	6.5e13	1e-11		0.01	0.2
11	4e9	1.6	5e12	6e-12		0	0

**Table 2**  
The simulation steps for obtaining the OSL dose response using a SAR-OSL technique. A single aliquot is used for all measurements. Steps 1–4 are a simulation of a “natural” quartz sample according to Bailey [6], with a variable natural burial dose  $D$ .

1	Geological dose irradiation of 1000 Gy at 1 Gy/s
2	Geological time–heat to 350 °C
3	Illuminate for 100 s at 200 °C
4	Burial dose $D$ at 20 °C at a natural dose rate of $3 \times 10^{-11}$ Gy/s
5	Irradiate sample with dose $D_i$ at a laboratory dose rate of 1 Gy/s
6	Preheat 10 s at 260 °C
7	Blue OSL for 100 s at 125 °C- Record OSL (0.1 s) signal ( $L$ )
8	Test dose $TD = 5$ Gy
9	Cutheat 20 s at 220 °C
10	Blue OSL for 100 s at 125 °C- Record OSL (0.1 s) signal ( $T$ )

Repeat steps 4–10 for the sequence of doses 0, 50, 100, 200, 800, and 1600 Gy to reconstruct the dose response curve  $L/T$  vs. dose.

each excitation stage in the simulations a relaxation period is introduced in which the temperature of the sample is kept constant at room temperature for 1 s after the excitation has stopped ( $R = 0$ ), and during which the concentrations of  $n_c$ ,  $n_v$  decay to negligible values. After each heating step the model simulates a cooling-down period with a constant cooling rate of  $\beta = -5$  °C s<sup>-1</sup>. A linear heating rate  $\beta = 5$  °C s<sup>-1</sup> is assumed during the simulation of the TL glow curves, so that  $T = T_0 + \beta \cdot t$  and  $R = 0$  during the read-out stage. During irradiation a value of  $R = 5 \times 10^7$  pairs/s is used to simulate an irradiation dose rate of 1 Gy/s.

**Table 3**  
The simulation steps for obtaining the isothermal-TL (ITL) dose response using a SAR-ITL technique. A single aliquot is used for all measurements. Steps 1–4 are identical to those in Table 1.

5	Irradiate sample with dose $D_i$ at a laboratory dose rate of 1 Gy/s
6	Preheat 10 s at 300 °C
7	Heat to 310 °C and hold for 600 s- Record ITL signal ( $L$ )
8	Test dose $TD = 50$ Gy
9	Preheat 10 s at 300 °C
10	Heat to 310 °C and hold for 600 s- Record ITL signal ( $T$ )
11	Optically stimulate for 40 s at 280 °C using blue diodes

Repeat steps 5–11 for the sequence of doses 0, 50, 100, 200, 800, and 1600 Gy to reconstruct the dose response curve  $L/T$  vs. dose.

**Table 4**  
The simulation steps for obtaining the equivalent dose (ED) using the SAR-OSL technique. A single aliquot is used for all measurements. Steps 1–4 are identical to those in Table 1.

1	Geological dose irradiation of 1000 Gy at 1 Gy/s
2	Geological time–heat to 350 °C
3	Illuminate for 100 s at 200 °C
4	Burial dose– $D$ at 20 °C at $3 \times 10^{-11}$ Gy/s
5	Irradiate sample with dose $D_i$
6	Preheat 10 s at 260 °C
7	Blue OSL for 100 s at 125 °C- Record OSL (0.1 s) signal ( $L$ )
8	Test dose $TD = 5$ Gy
9	Cutheat 20 s at 220 °C
10	Blue OSL for 100 s at 125 °C- Record OSL (0.1 s) signal ( $T$ )

Repeat steps 5–10 for a sequence of different regenerative doses e.g.  $D_i=(0, 500, 1000, 1500, 0, \text{and } 500 \text{ Gy})$  to reconstruct the dose response curve  $L/T$  vs. dose. Estimate ED using interpolation.

**Table 5**  
The simulation steps for obtaining the ED using the SAR-ITL technique. A single aliquot is used for all measurements. Steps 1–4 are identical to those in Table 1.

5	Irradiate sample with dose $D_i$ at a laboratory dose rate of 1 Gy/s
6	Preheat 10 s at 300 °C
7	Heat to 310 °C and hold for 600 s- Record ITL signal ( $L$ )
8	Test dose $TD = 50$ Gy
9	Preheat 10 s at 300 °C
10	Heat to 310 °C and hold for 600 s- Record ITL signal ( $T$ )
11	Optically stimulate for 40 s at 280 °C using blue diodes

Repeat steps 5–11 for a sequence of different regenerative doses e.g.  $D_i=(0, 500, 1000, 1500, 0, \text{and } 500 \text{ Gy})$  to reconstruct the ITL dose response curve  $L/T$  vs. dose. Estimate ED using interpolation.

### 5. Simulation of random natural variations in quartz samples

Our simulation method is similar to the published work by Bailey [7]. Specifically we simulate the experimentally observed variability in TL and OSL characteristics of quartz by assuming that all the fundamental transition probabilities in the model remain constant, while trap concentrations (parameters  $N_1, N_2, \dots, N_{11}$  in Table 1) are allowed to vary randomly within  $\pm 80\%$  from the values shown in Table 1. As discussed by Bailey [7] in p.304, some variation of the transition probabilities may also be present in natural samples, but this variation is expected to be relatively insignificant.

We use the parameters of the comprehensive model of Pagonis et al. [25] as our “standard” quartz model, and  $N = 300$  versions of the parameters were generated by randomly selecting concentration values within  $\pm 80\%$  of the original values, using uniformly distributed random numbers. For each of these variants the full sequence of irradiation and thermal history of the samples were simulated, and the two dating protocols were simulated in order to obtain an estimate of their relative intrinsic accuracy and precision. Even though our approach in this paper is similar to that of Bailey [7], our goals are different. We are interested in a comparative study of the dose responses of the TL and OSL signals, as well as in the various factors affecting the intrinsic accuracy and precision of the two simulated dating protocols. Furthermore, we present new simulations of the sensitivity changes occurring during application of the SAR-ITL technique not found previously in the literature.

An initial set of simulations was carried out using  $N = 300$  random concentration variants, and the results were compared with those obtained when using only  $N = 100$  variants. Comparison of the  $N = 300$  and  $N = 100$  results showed a very small improvement of less than 0.5% in the precision of the simulated results, while the corresponding accuracy of the simulations remained unaffected. On the basis of these initial results, it was decided to carry out the rest of the simulations for  $N = 100$  natural variants of the sample, for the sake of saving computation time. The computer code is written in Mathematica, and typical running times for 100 variations of the SAR-OSL or SAR-ITL techniques are  $\sim 40$  min on a PC. It was found necessary to use a solver for “stiff” differential equations in several of the simulations, and the Mathematica software switched automatically between a stiff and non-stiff solver whenever necessary.

It is emphasized that the intrinsic precision and accuracy simulated in this paper are only one part of the overall precision and accuracy encountered during experimental applications of the two protocols. For a detailed discussion of the various factors affecting the overall experimental accuracy and precision of the SAR-OSL technique the reader is referred to the detailed discussion in Duller [17].

### 6. Simulated dose response curves for the OSL and isothermal-TL signals

Fig. 2a shows the results of simulating the dose response of the OSL signal using a SAR-OSL protocol; the complete sequence of steps in the simulation is shown in Table 2. The result of Fig. 2a was obtained using the set of published kinetic parameters shown in Table 1, also found in Pagonis et al. [25]. The simulated dose response curves in Figs. 2a show that the OSL signal starts saturating at a dose of  $\sim 400$  Gy. The experimental data of Wang et al. [30] for quartz sample IEE209 are also shown in Fig. 2a for comparison purposes. This set of experimental data was obtained for a young IEE209 sample which had a natural dose of 3 Gy.

Fig. 2b shows the simulated dose responses using the SAR-ITL protocol, when either a single aliquot or multiple aliquots are used;

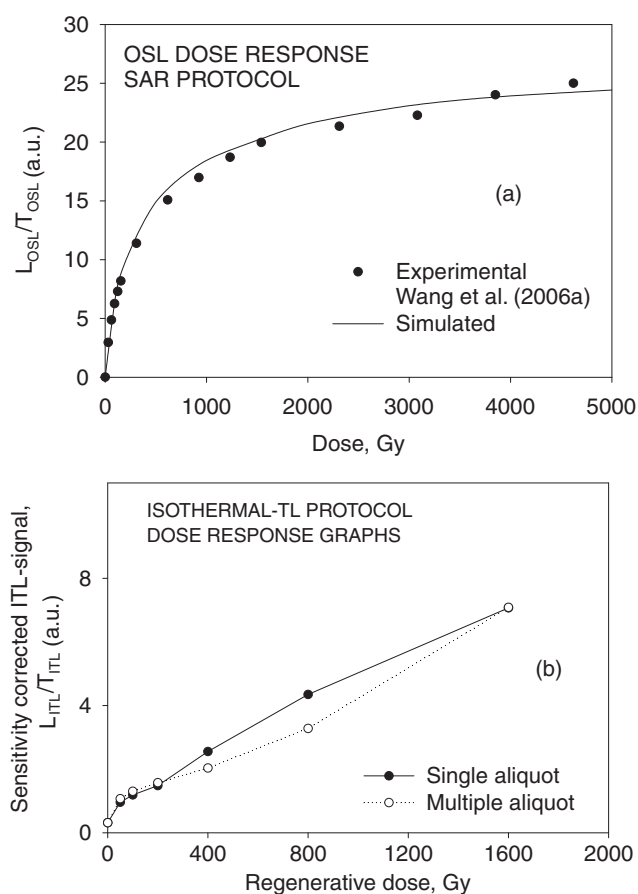


**Fig. 2.** (a) The simulated dose response of the OSL signal using a SAR-OSL protocol. The complete sequence of steps in the simulation is shown in Table 2 and the kinetic parameters used are shown in Table 1. The experimental data of Wang et al. [30] for quartz sample IEE209 are also shown for comparison purposes. (b) The simulated dose response of the isothermal-TL signal obtained using the SAR-ITL protocol, when either a single aliquot or multiple aliquots are used. The complete sequence of steps in this simulation is shown in Table 3. The simulated data in (b) are very similar in shape and in order of magnitude to published SAR-ITL dose response curves [29], their Fig. 4b).

the complete sequence of steps in this simulation is shown in Table 3. The single and multiple aliquot dose responses in Fig. 2b are very similar to each other, with the single aliquot data appearing systematically higher than the multiple aliquot data at higher doses. This is most likely due to the total doses being much larger in the case of single aliquot measurements, leading to corresponding larger isothermal-TL signals. The simulated data in Fig. 2b are similar in shape and of the same order of magnitude as published SAR-ITL dose response curves [29], their Fig. 4b). Comparison of the dose response curves in Figs. 2a and b shows that the OSL signal starts saturating at a dose of  $\sim 400$  Gy, while the corresponding isothermal-TL signal shows no sign of saturation even at a dose of 1600 Gy.

The simulation of the OSL dose response in Fig. 2a was repeated using the 100 variants of the natural quartz sample described in previous sections, and the resulting dose response curves were averaged. The result of averaging these 100 dose response curves are shown in Fig. 3a for the SAR-OSL protocol. The y-axis in Fig. 3a represents the average  $(L/T)_{average}$  or mean of the 100  $L/T$  values obtained at each dose. At each dose we evaluate the standard deviation  $\sigma$  of the 100  $L/T$  values. The error of the average value  $(L/T)_{average}$  is represented by the standard deviation of the mean  $\sigma_{mean} = \sigma/\sqrt{N}$  (in our case  $N = 100$ ).

The error bars shown in Fig. 3a therefore correspond to this standard deviation of the mean  $\sigma_{mean} = \sigma/\sqrt{N}$ , and the value of

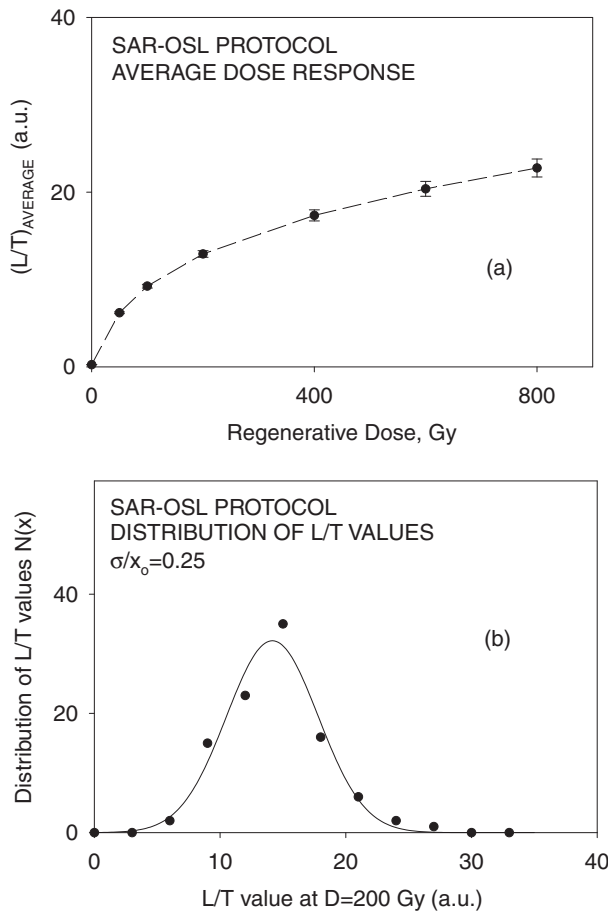


**Fig. 3.** (a) The result of averaging 100 simulated dose response curves for the SAR-OSL protocol using 100 variants of the natural quartz sample, as discussed in the text. The y-axis represents the average  $(L/T)_{\text{average}}$  of the 100  $L/T$  values obtained at each dose. The error bars shown correspond to the standard deviation of the mean  $\sigma_{\text{mean}} = \sigma/\sqrt{N}$ , where  $\sigma$  is the standard deviation of the 100  $L/T$  values at each dose (in our case  $N = 100$ ). The value of  $\sigma_{\text{mean}}$  provides an estimate of the intrinsic precision of the  $L/T$  measurements at the various doses, and gets increasingly larger at higher doses. This result is similar to the simulated results of Bailey [7]. (b) A typical example of the distribution of the sensitivity corrected  $L/T$  signals at a dose of 200 Gy, shown in the form of a histogram. The solid line represents a fitted Gaussian distribution according to Eq. (1), centered at  $x_0 = (L/T)_{\text{average}} = 14.2$  (a.u.) and with a standard deviation of the data  $\sigma = 3.65$  (a.u.). The ratio  $\sigma/x_0 = 0.25$  provides an estimate of the intrinsic precision of the  $L/T$  measurements at a dose  $D = 200$  Gy.

$\sigma_{\text{mean}}$  provides an estimate of the precision of the average  $L/T$  measurements at the various doses. As can be seen in Fig. 3a, the simulated precision  $\sigma_{\text{mean}}$  gets increasingly larger at higher doses. These results are similar to the simulated results of Bailey [7] for the SAR-OSL protocol.

A typical example of the distribution of the sensitivity corrected  $L/T$  signals at a dose of 200 Gy is shown in the form of a histogram in Fig. 3b. The resulting Gaussian distributions of the  $L/T$  values were fitted with a Gaussian distribution  $N(x)$  of the form:

$$N(x) = A \exp\left(-\frac{(x - x_0)^2}{2\sigma^2}\right), \quad (1)$$

where  $x$  is the sensitivity corrected SAR-OSL  $L/T$  signal at a dose of 200 Gy. The constant  $A$  in this equation represents the number of variants at the peak of the distribution which is centered at  $x_0 = (L/T)_{\text{average}}$ , and the Gaussian distribution has a standard deviation of the data given by  $\sigma$ . The fitted Gaussian distribution for the SAR-OSL technique in Fig. 3b is centered at  $x_0 = (L/T)_{\text{average}} = 14.2$

(a.u.) and the standard deviation of the data is  $\sigma = 3.65$  (a.u.). The corresponding value of  $\sigma_{\text{mean}} = \sigma/\sqrt{N} = 0.365$  (a.u.). The ratio  $\sigma/x_0 = 0.25$  provides an estimate of the intrinsic precision of the  $L/T$  measurements at a dose  $D = 200$  Gy.

A similar set of simulations were carried out for the isothermal-TL protocol, and the results are shown in Figs. 4a and b. The result of averaging the 100 dose response curves are shown in Fig. 4a, with the error bars corresponding once again to  $\sigma_{\text{mean}}$ , the standard deviation of the mean. As can be seen in Fig. 4a, the simulated intrinsic precision of the isothermal-TL protocol gets larger at higher doses, similar to the case of the SAR-OSL protocol shown in Fig. 3a.

Fig. 4b shows a typical example of the distribution of the sensitivity corrected  $L/T$  signals at a dose of 200 Gy, with a fitted Gaussian distribution  $N(x)$ . In the case of the SAR-ITL protocol the fitted Gaussian distribution is centered at  $x_0 = (L/T)_{\text{average}} = 1.79$  and the standard deviation of the data is  $\sigma = 0.39$ . The ratio  $\sigma/x_0 = 0.22$  provides an estimate of the precision of the  $L/T$  measurements in the SAR-ITL protocol at a dose  $D = 200$  Gy. This value is very close to the corresponding value of  $\sigma/x_0 = 0.25$  obtained in Fig. 3b for the

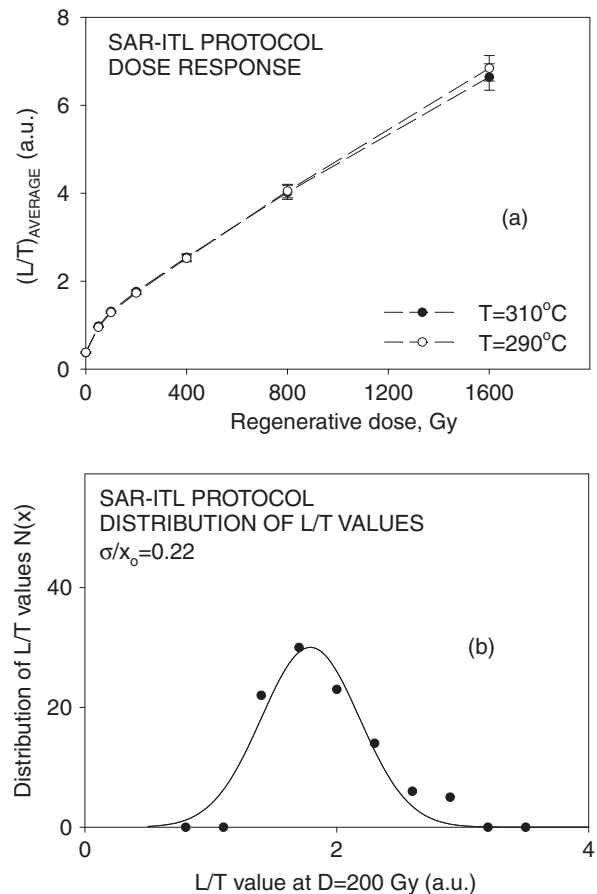


**Fig. 4.** (a) The simulated result of averaging 100 dose response curves for the SAR-ITL protocol using 100 variants of the natural quartz sample, as discussed in the text. The y-axis represents the average  $(L/T)_{\text{average}}$  of the 100  $L/T$  values obtained at each dose. The error bars shown correspond to the standard deviation of the mean  $\sigma_{\text{mean}} = \sigma/\sqrt{N}$ . The value of  $\sigma_{\text{mean}}$  provides an estimate of the precision of the  $L/T$  measurements at the various doses, and gets increasingly larger at higher doses. (b) A typical example of the distribution of the sensitivity corrected  $L/T$  signals for the SAR-ITL protocol at a dose of 200 Gy, shown in the form of a histogram. The fitted Gaussian distribution according to equation (1), centered at  $x_0 = (L/T)_{\text{average}} = 1.79$  (a.u.) and with a standard deviation of the data  $\sigma = 0.39$  (a.u.). The ratio  $\sigma/x_0 = 0.22$  provides an estimate of the intrinsic precision of the  $L/T$  measurements at a dose  $D = 200$  Gy.

SAR-OSL protocol, indicating that the intrinsic precision of the two protocols is very similar at a regenerative dose of  $D = 200$  Gy.

### 7. Simulations of the SAR-OSL and SAR-ITL dating protocols

Fig. 5a shows a typical example of simulating the SAR-OSL protocol developed during the past 10 years [34]. The detailed steps in this simulation are shown in Table 2. The five regenerative doses used were 0, 160, 200, 240, 0 and 160 Gy, and the test dose used was 5 Gy. The preheat temperature used in the SAR protocol simulation was 10 s at 260 °C for the regenerative dose measurements, and the cut-heat used for the test dose measurements was 20 s at 220 °C. The sensitivity corrected signals  $L/T$  shown in Fig. 5a were used to reconstruct the dose response curve, and as usual an interpolation was used for estimating the accrued dose ED by the sample. In the example shown in Fig. 5a the recycling ratio was 1.03, the zero-dose was 0.0002 and the recovered dose was ED = 230 Gy.

A typical example of simulating 100 variants within the SAR-OSL technique for a dose  $D = 200$  Gy are shown in Fig. 5b, and this is fitted with a Gaussian distribution functions shown as a solid line. The resulting Gaussian distributions of the ED values were fitted with a Gaussian expression  $N(D)$  of the form:

$$N(D) = A \exp\left(-\frac{(D - D_{\text{average}})^2}{2\sigma^2}\right), \quad (2)$$

where  $D$  is the ED value obtained from the SAR-OSL protocol for each of the 100 sample variants. The constant  $A$  represents the number of variants at the peak of the distribution which is centered at  $D_{\text{average}}$ , and the Gaussian distribution has a standard deviation of the data given by  $\sigma$ . The fitted Gaussian distribution for the SAR-OSL technique in Fig. 5b is centered at  $D_{\text{average}} = 213$  Gy and the standard deviation of the data is  $\sigma = 21$  Gy. The ratio  $\sigma/D_{\text{average}} = 21/213 = 0.10$  provides an estimate of the intrinsic precision of the SAR-OSL protocol at the burial dose of  $D = 200$  Gy.

Fig. 5c shows the results of the SAR-OSL simulation for burial doses in the range 0–400 Gy. The error bars shown in Fig. 5c correspond to the standard deviation of the mean ED values  $\sigma_{\text{mean}} = \sigma/\sqrt{N}$ , where  $\sigma$  represents the standard deviation of the 100 ED values obtained at each dose and  $N = 100$ . The value of  $\sigma_{\text{mean}}$  provides an estimate of the simulated intrinsic precision of the SAR-OSL protocol at the various doses. As can be seen in Fig. 5c, the simulated precision  $\sigma_{\text{mean}}$  gets increasingly worse at higher doses. Fig. 5c also shows that the SAR-OSL technique can reproduce doses accurately in the complete dose region with an intrinsic accuracy better than 6%. As may be expected, the accuracy and precision of the SAR-OSL technique get slightly worse at higher doses, due to the “flattening” of the shape of the OSL dose response curves after ~400 Gy, as shown in Fig. 2a.

Fig. 6 shows results similar to those in Fig. 5, for the case of the SAR-ITL dating protocol. In the example shown in Fig. 6a, the recycling ratio was 1.07, the zero-dose was 0.003 and the recovered dose was ED = 168 Gy. A typical example of simulating 100 variants within the SAR-ITL technique for a burial dose  $D = 200$  Gy are shown in Fig. 6b, and the fitted Gaussian distribution function is shown as a solid line and is centered at  $D_{\text{average}} = 229$  Gy and the standard deviation of the data is  $\sigma = 31$  Gy. The ratio  $\sigma/D_{\text{average}} = 0.14$  provides an estimate of the intrinsic precision of the SAR-ITL protocol at the burial dose of  $D = 200$  Gy. By comparing the Gaussian distributions in Figs. 5b and 6b, it can be seen that the SAR-OSL protocol is both more accurate and more precise than the SAR-ITL protocol, at least for the example of  $D = 200$  Gy shown here.

Fig. 6c shows the results of the SAR-ITL simulation for paleodoses in the range 0–800 Gy. The error bars shown in Fig. 6c correspond once more to the standard deviation of the mean ED

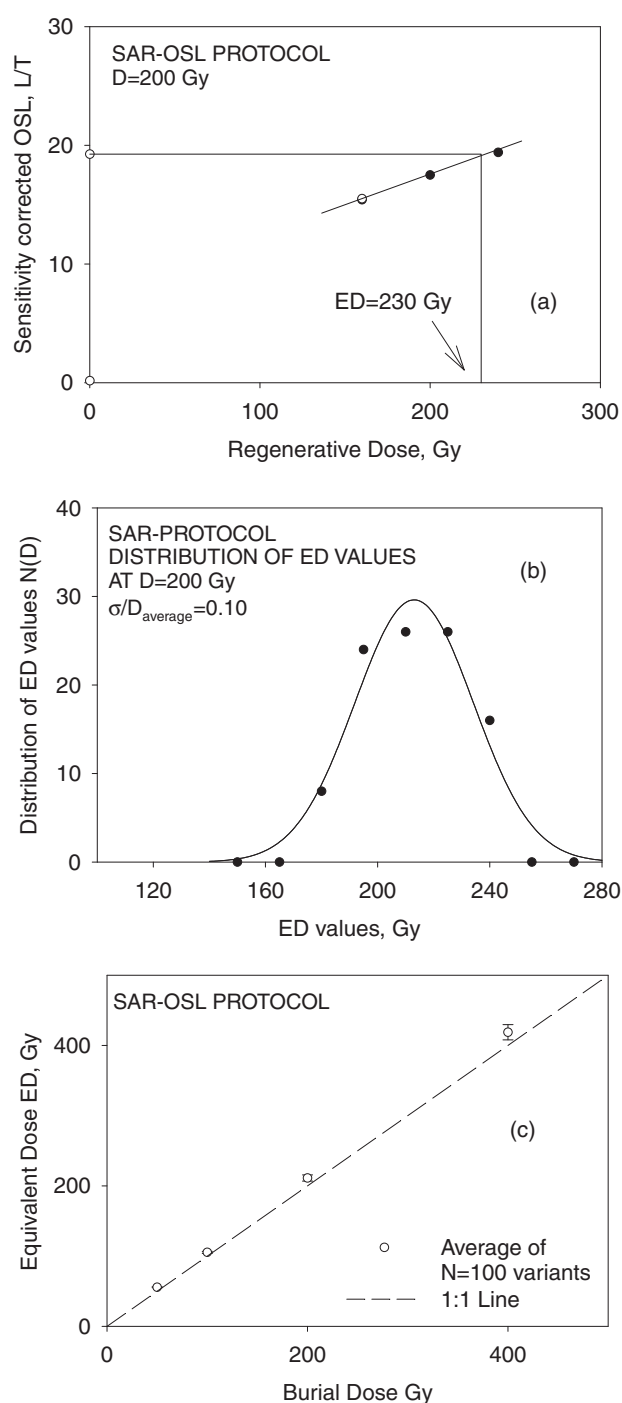
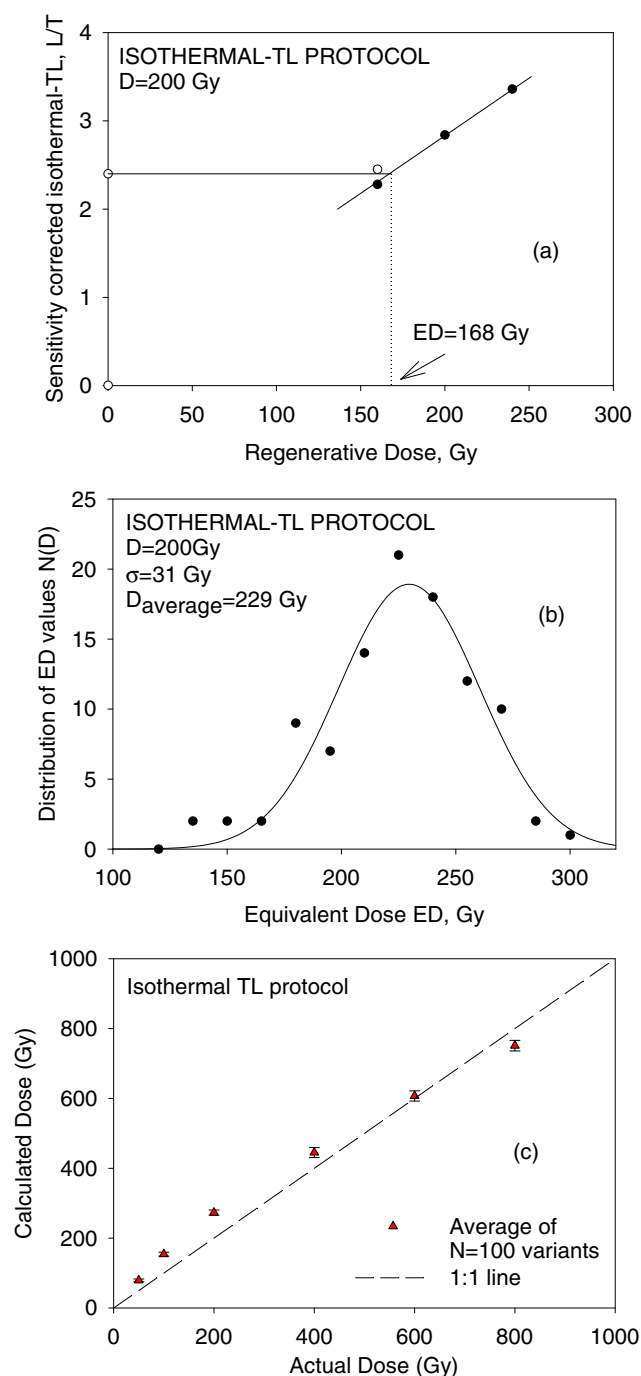


Fig. 5. (a) A typical example of simulating the SAR-OSL protocol; the steps in this simulation are shown in Table 4. The sensitivity corrected signals  $L/T$  are used to reconstruct the dose response curve, and interpolation was used for estimating the equivalent dose ED by the sample. In this example the recycling ratio was 1.03, the zero-dose was 0.0002 and the recovered dose was ED = 230 Gy. (b) A typical example of simulating 100 variants within the SAR-OSL technique for a dose  $D = 200$  Gy is shown as a histogram. The fitted Gaussian distribution functions according to Eq. (2) is centered at  $D_{\text{average}} = 213$  Gy and the standard deviation of the data is  $\sigma = 21$  Gy. The ratio  $\sigma/D_{\text{average}} = 21/213 = 0.10$  provides an estimate of the intrinsic precision of the SAR-OSL protocol at the burial dose of  $D = 200$  Gy. (c) The results of the SAR-OSL simulation for burial doses in the range 0–400 Gy. The error bars correspond to the standard deviation of the mean ED values  $\sigma_{\text{mean}} = \sigma/\sqrt{N}$ , where  $\sigma$  represents the standard deviation of the 100 ED values obtained at each dose, and  $N = 100$ . The value of  $\sigma_{\text{mean}}$  provides an estimate of the simulated intrinsic precision of the SAR-OSL protocol at the various doses. The simulated data in this Figure shows that  $\sigma_{\text{mean}}$  gets increasingly worse at higher doses, and that the SAR-OSL technique can reproduce doses accurately in this dose region with accuracy better than 6%.



**Fig. 6.** (a) A typical example of simulating the SAR-ITL protocol. The steps in this simulation are shown in Table 5. The sensitivity corrected signals  $L/T$  are used to reconstruct the dose response curve, and interpolation was used for estimating the equivalent dose  $ED$  by the sample. In this example the recycling ratio was 1.07, the zero-dose was 0.003 and the recovered dose was  $ED = 168$  Gy. (b) A typical example of simulating 100 variants within the SAR-ITL technique for a dose  $D = 200$  Gy is shown as a histogram. The fitted Gaussian distribution functions according to Eq. (2) is centered at  $D_{\text{average}} = 229$  Gy and the standard deviation of the data is  $\sigma = 31$  Gy. The ratio  $\sigma/D_{\text{average}} = 0.14$  provides an estimate of the intrinsic precision of the SAR-ITL protocol at the burial dose of  $D = 200$  Gy. Comparison of Figs. 5b and 6b shows that the SAR-ITL data shows a much larger scattering than the corresponding SAR-OSL data in Fig. 5b. (c) The results of the SAR-ITL simulation for burial doses in the range 0–800 Gy. The error bars correspond to the standard deviation of the mean  $ED$  values  $\sigma_{\text{mean}} = \sigma/\sqrt{N}$ . The value of  $\sigma_{\text{mean}}$  provides an estimate of the simulated intrinsic precision of the SAR-ITL protocol at the various doses. The simulated data in this figure shows that the SAR-ITL protocol systematically overestimates the burial dose in the range 0–700 Gy, in agreement with several experimental studies discussed in the text.

values  $\sigma_{\text{mean}} = \sigma/\sqrt{N}$ , where  $\sigma$  represents the standard deviation of the  $N = 100$   $ED$  values obtained at each dose. As can be seen in Fig. 6c, the simulated intrinsic precision  $\sigma_{\text{mean}}$  for SAR-ITL gets increasingly worse at higher doses, as was also the case for the SAR-OSL protocol shown in Fig. 5c. However, it is also noted that the isothermal-TL data shows a much larger scattering of the data in Fig. 6b than the corresponding SAR-OSL data in Fig. 5b. This result of scattering of the data being larger for the SAR-ITL technique was verified at all other burial doses.

An important observation from Figs. 5c and 6c is that the SAR-ITL protocol systematically overestimates the burial dose in the range 0–700 Gy, while the SAR-OSL protocol produces the correct burial doses in the dose range 0–400 Gy (with a very slight overestimation for  $D > 200$  Gy). This simulated overestimation of the burial doses by the SAR-ITL protocol is in good agreement with several experimental studies reported in the introduction to this paper [12,19]. This systematic failure of the SAR-ITL protocol based on the 310 °C ITL signal is examined further in a subsequent section which simulates the sensitivity changes occurring during the two protocols.

## 8. Simulations of various experimental factors affecting the SAR-ITL protocol

In this section we simulate the accuracy of the SAR-ITL protocol by changing various experimental factors. We start by examining the accuracy of the SAR-ITL protocol when the isothermal-TL signal is measured at temperatures of 270, 290 and 310 °C. The simulated solid circles in Fig. 7a show that using a lower measurement temperature of 270 °C (solid circles) improves the accuracy of the SAR-ITL protocol, at least for doses up to 400 Gy. The solid circles corresponding to 270 °C lie closer to the 1:1 line than the open circles and the triangles, at least up to  $\sim 400$  Gy. For large doses  $\sim 800$  Gy all three ITL signals underestimate the burial dose significantly.

Vandenbergh et al. [29] examined the effect of using a large test dose during the SAR-ITL protocol, and found that at least in one case the use of a larger dose improved the accuracy of the protocol (see their Fig. 6). We simulated the effect of the test dose on the accuracy of the SAR-ITL protocol, with the results shown in Fig. 7b. The simulated solid circles in Fig. 7b correspond to a test dose of 400 Gy, and they indicate an improved accuracy over the triangles (test dose = 50 Gy), at least for doses between 100 and 400 Gy. At low doses of 50 Gy and larger doses of 600 Gy, the smaller test dose produces more accurate results. These simulated results indicate that the magnitude of the test dose should be examined carefully during applications of the SAR-ITL protocol, since it can affect the accuracy at various burial doses.

## 9. Simulations of sensitivity changes occurring during successive irradiations with the same dose

Wintle and Murray [34] suggested carrying out tests of sensitivity changes occurring during the SAR-OSL protocol, by carrying out successive cycles of sample irradiation with the same dose  $D$ , followed by measurement of the sensitivity corrected OSL  $L/T$  signal. In such sensitivity tests one plots the test dose OSL signal (termed the  $T$ -signal) as a function of the corresponding uncorrected OSL signal (termed the  $L$ -signal). Such graphs of  $L$  vs.  $T$  should be linear and should pass through the origin of the graph. During the past few years several authors have published such  $L-T$  graphs for the SAR-OSL protocol, but there has been no systematic simulation study of this type of measurement. Furthermore, there are no published simulated  $L-T$  graphs of the SAR-ITL protocol in the literature. In this section we describe such  $L-T$  simulations for the

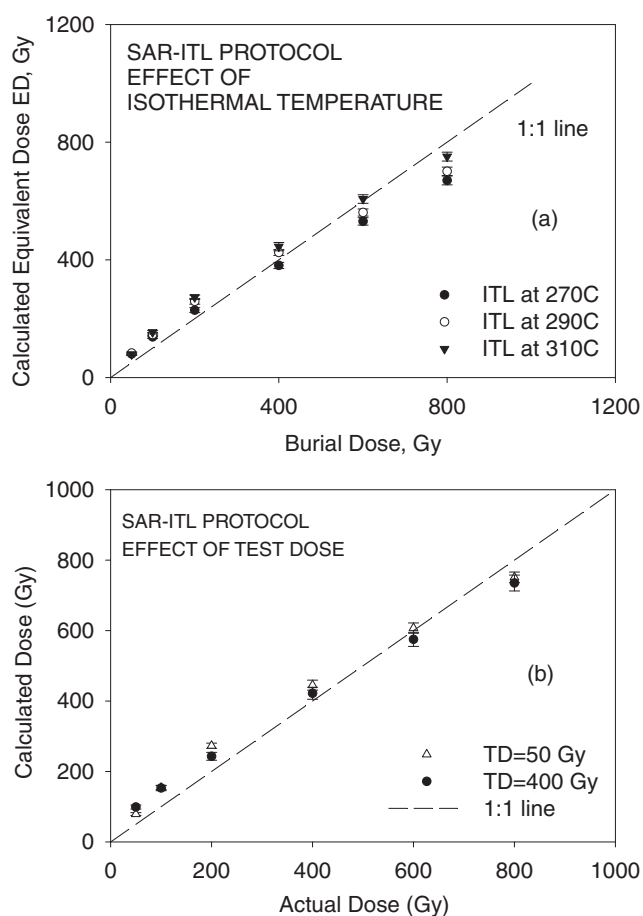


**Fig. 7.** (a) Simulation of the accuracy of the SAR-ITL protocol when the isothermal-TL signal is measured at temperatures of 270, 290 and 310 °C. The data in this figure shows that using a lower measurement temperature of 270 °C (solid circles) improves the accuracy of the SAR-ITL protocol, at least for doses up to 400 Gy. The solid circles corresponding to 270 °C lie closer to the 1:1 line than the open circles and the triangles, at least up to ~400 Gy. For large doses of ~800 Gy all three ITL signals underestimate the burial dose significantly. (b) Simulation of the effect of the test dose on the accuracy of the SAR-ITL protocol. The solid circles corresponding to a test dose of 400 Gy indicate an improved accuracy over the triangles (test dose = 50 Gy), at least for doses between 100 and 400 Gy. At low doses of 50 Gy and larger doses of 600 Gy, the smaller test dose produces more accurate results.

SAR-OSL and SAR-ITL protocols; our goal is to examine what experimental factors could be affecting the  $L$ - $T$  graphs, and to carry out a comparison of these types of graphs between the two protocols.

We simulated  $L$ - $T$  tests for both the SAR-OSL protocol and the SAR-ITL protocol, and typical results are shown in Figs. 8 and 9. Fig. 8a shows  $L$ - $T$  graphs for the SAR-OSL protocol consisting of 10 cycles of a regenerative dose  $D = 20$  Gy, using the parameters in Table 1. Two simulated examples are shown in this Figure. The first example is for a quartz sample that was optically bleached before the successive irradiation cycles, and the second example is for an unbleached sample. Both  $L$ - $T$  graphs are seen to be linear and passing through the origin. Fig. 8b shows the corresponding ratio  $L/T$  obtained from the data in Fig. 8a, showing that for both optically bleached and unbleached samples the SAR-OSL protocol provides appropriate corrections of sensitivity changes occurring between successive irradiations. It is noted that the SAR-OSL sensitivity  $T$  changes by ~40% during the 10 cycles in Fig. 8.

Fig. 9 shows an example of simulating the sensitivity test for the SAR-ITL protocol, consisting of 10 cycles of a regenerative dose  $D = 1000$  Gy. This simulation was carried out using the parameters in Table 1 and using a test dose  $TD = 50$  Gy in the protocol. The  $L$ - $T$  graphs are seen to be linear and to pass closely (but not exactly)

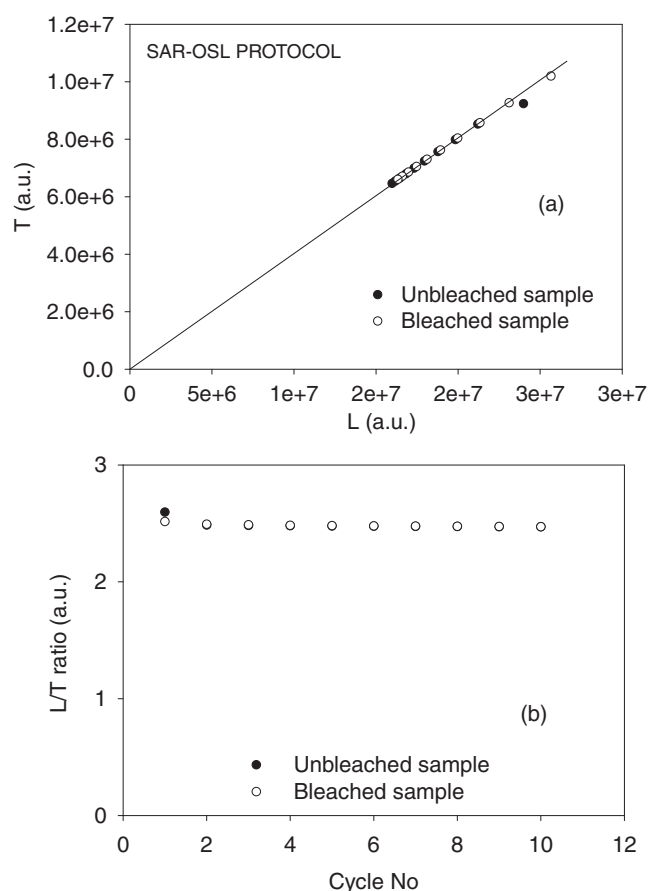


**Fig. 8.** Simulated successive cycles of sample irradiation with the same dose  $D$ , followed by measurement of the sensitivity corrected SAR-OSL  $L/T$  signal. Such graphs of  $L$  vs.  $T$  should be linear and should pass through the origin of the graph. (a) Simulated  $L$ - $T$  graphs for the SAR-OSL protocol consisting of 10 cycles of a regenerative dose  $D = 20$  Gy, using the parameters in Table 1. Two examples are shown, for an optically bleached sample and for an optically unbleached sample. Both  $L$ - $T$  graphs are seen to be linear and passing through the origin. (b) The corresponding  $L/T$  ratios obtained from the data in (a) shows that the SAR-OSL protocol provides appropriate corrections of sensitivity changes occurring between successive irradiations, for both optically bleached and unbleached samples.

through the origin. Fig. 9b shows the corresponding ratio  $L/T$  obtained from the data in Fig. 9a, showing a very large sensitivity-change occurring during the first application of the SAR-ITL protocol. This sensitivity change does not get corrected by the SAR-ITL protocol, and is most likely the main reason that experimental applications of the SAR-ITL protocol fail for some quartz samples. The simulated sensitivity change in Fig. 9b is in good agreement with the reported failures of the SAR-ITL protocol discussed in a previous section.

We have also carried out simulations similar to the one shown in Fig. 9a, by using several different test doses in the SAR-ITL protocol. The goal here was to ascertain whether the initial sensitivity-change occurring during the protocol depends on the size of the test dose. This is shown to be the case for the simulated data in Fig. 10. Larger test doses result in smaller initial sensitivity changes during the SAR-ITL protocol, and the SAR-ITL protocol may be expected to be more accurate when large test doses are employed.

Finally we investigated whether the size of the test doses affects the shape of the  $L$ - $T$  graphs. The results of these simulations are shown in Fig. 11. Fig. 11a shows that linear  $L$ - $T$  graphs are obtained for all 3 test doses  $TD = 50, 130$  and  $250$  Gy. However, the y-intercept of these graphs becomes larger for larger test doses. This effect is shown more clearly in Fig. 11b, in which the  $L$ - $T$  graphs are normalized to the first (non-natural dose) point in the sequence of

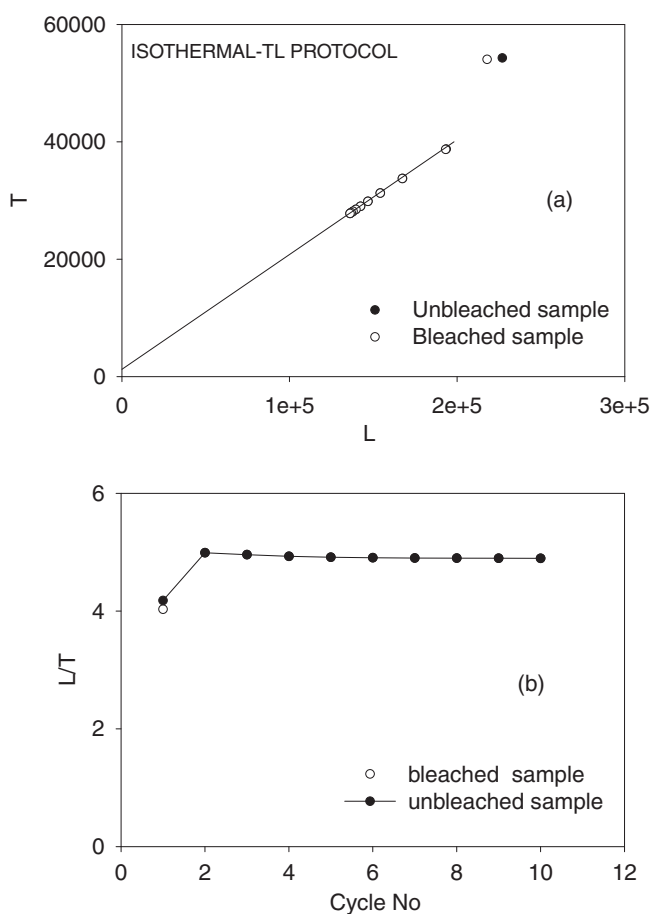


**Fig. 9.** Simulated successive cycles of sample irradiation with the same dose  $D$ , followed by measurement of the sensitivity corrected SAR-ITL signal. Such graphs of  $L$  vs.  $T$  should be linear and should pass through the origin of the graph. (a) Simulated  $L$ - $T$  graphs for the SAR-OSL protocol consisting of 10 cycles of a regenerative dose  $D = 1000$  Gy, using the parameters in Table 1. When the first measurement near the top of this graph is ignored, the  $L$ - $T$  graphs are seen to be linear and passing close to the origin. (b) The corresponding ratio  $L/T$  obtained from the data in (a) shows that the SAR-ITL protocol does not provide appropriate correction of sensitivity changes occurring between successive irradiations. This is due to a large sensitivity-change occurring during the first cycle, as reported in several experimental studies discussed in the text.

doses. We conclude that the size of the test dose affects not only the accuracy of the SAR-ITL protocol, but also affects the shape and y-intercept of the  $L$ - $T$  graphs.

### 10. Conclusions

The comprehensive quartz model of Pagonis et al. [25] was used successfully in this paper to simulate the complete sequence of experimental steps taken during the SAR-OSL and SAR-ITL protocols. The first technique is based on OSL signals, while the second one is based on measurements of isothermal-TL signals. The results of the simulations show that the SAR-OSL protocol is in general more accurate and more precise, while the SAR-ITL protocol is more sensitive to the specific experimental conditions. One may anticipate this result on physical grounds, since thermal signals will contain in general contributions from all traps and centers in the quartz sample, while fewer optically sensitive traps will contribute to the SAR-OSL signals.

One important result of the simulations is a demonstration of the sensitivity-change occurring between successive dosing of a quartz sample. In the case of the SAR-OSL protocol the sensitivity

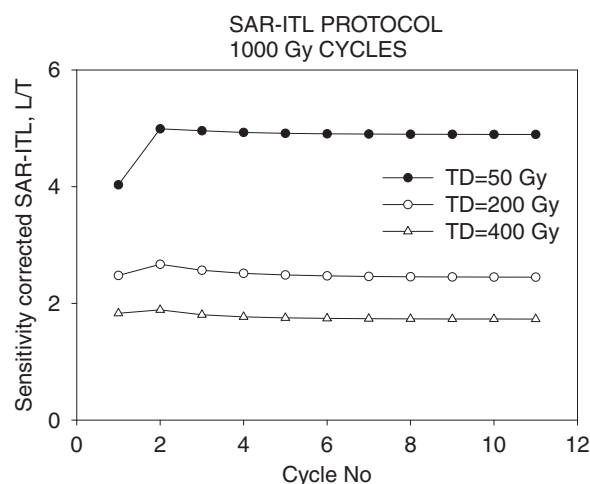


**Fig. 10.** Simulations similar to the ones shown in Fig. 9b are carried out using several different test doses, showing that the initial sensitivity-change occurring during the SAR-ITL protocol depends on the size of the test dose. Using large test doses decreases the sensitivity-change occurring during the first cycle in the SAR-ITL protocol, and therefore leads to better accuracy.

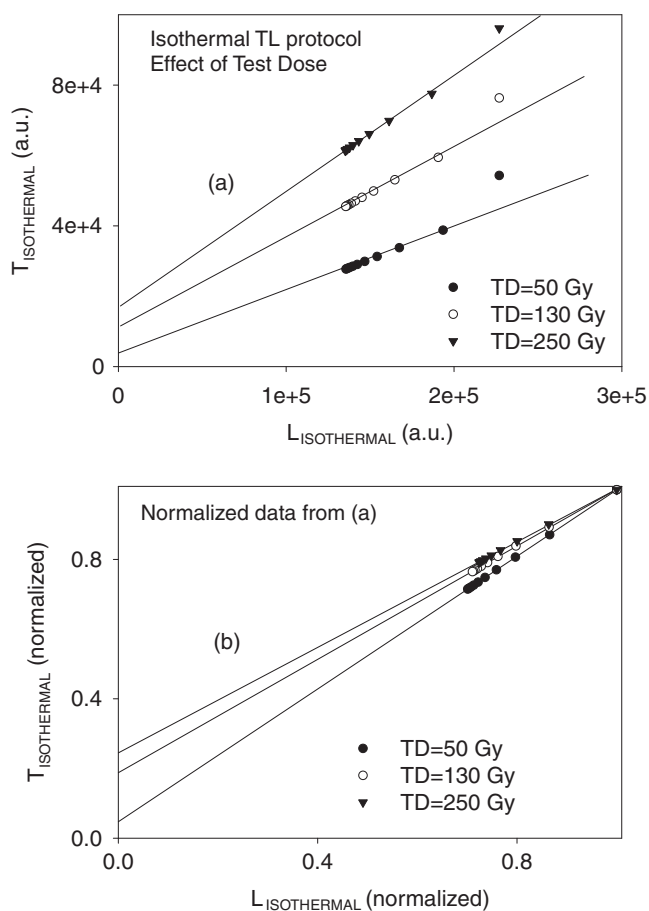


**Fig. 11.** The effect of the test dose size (TD) on the  $L$ - $T$  graphs for the SAR-ITL protocol. (a) The  $L$ - $T$  graphs obtained for 3 different test doses TD = 50, 130 and 250 Gy during application of the SAR-ITL protocol. The y-intercept of these graphs becomes larger for larger test doses. (b) The effect in (a) is shown more clearly by normalizing the  $L$ - $T$  graphs to the first point in the sequence of doses. The simulated data in this Figure shows that the size of the test dose affects the slope and y-intercept of the  $L$ - $T$  graphs.

changes are accounted for correctly, as shown in Fig. 8b. However, in the case of the SAR-ITL protocol these changes are of a fundamentally different nature, and cannot be accounted for correctly by the SAR procedure. However, it was found that in some cases it may be possible to minimize these sensitivity changes during the SAR-ITL protocol, by the use of rather large test doses, as shown in Fig. 10.

## References

- [1] G. Adamiec, M. Garcia-Talavera, R.M. Bailey, P. Iniguez de la Torre, Application of a genetic algorithm to finding parameter values for numerical stimulation of quartz luminescence, *Geochronometria* 23 (2004) 9–14.
- [2] G. Adamiec, A. Bluszcz, R. Bailey, M. Garcia-Talavera, Finding model parameters: genetic algorithms and the numerical modeling of quartz luminescence, *Radiat. Meas.* 41 (2006) 897–902.
- [3] G. Adamiec, R.M. Bailey, X.L. Wang, A.G. Wintle, The mechanism of thermally transferred optically stimulated luminescence in quartz, *J. Phys. D Appl. Phys.* 41 (2008) 135503.
- [4] G. Adamiec, G.A.T. Duller, H.M. Roberts, A.G. Wintle, Improving the TT-OSL SAR protocol through source trap characterization, *Radiat. Meas.* 45 (2010) 768–777.
- [5] M.J. Aitken, *Thermoluminescence Dating*, Academic press, London, 1985 (ISBN 012-0463806).
- [6] R.M. Bailey, Towards a general kinetic model for optically and thermally stimulated luminescence in quartz, *Radiat. Meas.* 33 (2001) 17–45.
- [7] R.M. Bailey, Paper I – simulation of dose absorption in quartz over geological timescales and its implications for the precision and accuracy of optical dating, *Radiat. Meas.* 38 (2004) 299–310.
- [8] R.M. Bailey, S.J. Armitage, S. Stokes, An investigation of pulsed-irradiation regeneration of quartz OSL and its implications for the precision and accuracy of optical dating (Paper II), *Radiat. Meas.* 39 (2005) (2005) 347–359.
- [9] I.K. Bailiff, The pre-dose technique, *Radiat. Meas.* 23 (1994) 471–479.
- [10] I.K. Bailiff, Retrospective dosimetry with ceramics, *Radiat. Meas.* 27 (1997) 923–941.
- [11] J.K. Bailiff, L. Botter-Jensen, V. Correcher, A. Delgado, H.Y. Göksu, H. Jungner, S.A. Petrov, Absorbed dose evaluation in retrospective dosimetry: methodological developments using quartz, *Radiat. Meas.* 32 (2000) 609–613.
- [12] J.P. Buylaert, A.S. Murray, S. Huot, M.G.A. Friend, D. Vandenberghe, F. De Corte, P. Van den haute, A comparison of quartz OSL and isothermal TL measurements on Chinese loess, *Radiat. Prot. Dosim.* 119 (2006) 474–478.
- [13] R. Chen, P.L. Leung, Processes of sensitization of thermoluminescence in insulators, *J. Phys. D: Appl. Phys.* 31 (1998) 2628–2635.
- [14] R. Chen, P.L. Leung, Modeling the pre-dose effect in thermoluminescence, *Radiat. Prot. Dosim.* 84 (1999) 43–46.
- [15] G. Chen, A.S. Murray, S.H. Li, Effect of heating on the quartz dose–response curve, *Radiat. Meas.* 33 (2001) 59–63.
- [16] J.H. Choi, A.S. Murray, C.S. Cheong, D.W. Hong, H.W. Chang, Estimation of equivalent dose using quartz isothermal TL and the SAR procedure, *Quat. Geochronol.* 1 (2006) 101–108.
- [17] Duller, Assessing the error on equivalent dose estimates derived from single aliquot regenerative dose measurements, *Ancient TL* 25 (2007) 15–24.
- [18] A. Galli, M. Martini, C. Montanari, L. Panzeri, E. Sibilia, TL of fine-grain samples from quartz-rich archaeological ceramics: dosimetry using the 110 and 210 C TL peaks, *Radiat. Meas.* 41 (2006) 1009–1014.
- [19] S. Huot, J.P. Buylaert, A.S. Murray, Isothermal thermoluminescence signals from quartz, *Radiat. Meas.* 41 (2006) 796–802.
- [20] M. Jain, L. Bøtter-Jensen, A.S. Murray, P.M. Denby, S. Tsukamoto, M.R. Gibling, Revisiting TL: dose measurement beyond the OSL range using SAR, *Ancient TL* 23 (2005) 9–24.
- [21] M. Jain, G.A.T. Duller, A.G. Wintle, Dose response, thermal stability and optical bleaching of the 310oC isothermal TL signal in quartz, *Radiat. Meas.* 42 (2007) 1285–1293.
- [22] S.W.S. McKeever, N. Agersnap Larsen, L. Bøtter-Jensen, V. Mejdahl, *Radiat. Meas.* 27 (1997) 75–82.
- [23] V. Pagonis, H. Carty, Simulation of the experimental pre-dose technique for retrospective dosimetry in quartz, *Radiat. Prot. Dosim.* 109 (2004) 225–234.
- [24] V. Pagonis, G. Kitis, R. Chen, Applicability of the Zimmerman predose model in the thermoluminescence of predosed and annealed synthetic quartz samples, *Radiat. Meas.* 37 (2003) 267–274.
- [25] V. Pagonis, A.G. Wintle, R. Chen, X.L. Wang, A theoretical model for a new dating protocol for quartz based on thermally transferred OSL (TT-OSL), *Radiat. Meas.* 43 (2008) 704–708.
- [26] V. Pagonis, E. Balsamo, C. Barnold, K. Duling, S. McCole, Simulations of the predose technique for retrospective dosimetry and authenticity testing, *Radiat. Meas.* 43 (2008) 1343–1353.
- [27] E.J. Rhodes, Quartz single grain OSL sensitivity distributions: implications for multiple grain single aliquot dating, *Geochronometria* 26 (2007) 19–29.
- [28] J.W. Thompson, Accuracy, precision, and irradiation time for Monte Carlo simulations of single aliquot regeneration (SAR) optically stimulated luminescence (OSL) dosimetry measurements, *Radiat. Meas.* 42 (2007) 1637–1646.
- [29] D.A.G. Vandenberghe, M. Jain, A.S. Murray, Equivalent dose determination using a quartz isothermal TL signal, *Radiat. Meas.* 44 (2009) 439–444.
- [30] X.L. Wang, Y.C. Lu, A.G. Wintle, Recuperated OSL dating of fine grained quartz in Chinese loess, *Quat. Geochronol.* 1 (2006) 89–100.
- [31] X.L. Wang, A.G. Wintle, Y.C. Lu, Thermally transferred luminescence in fine-grained quartz from Chinese loess: basic observations, *Radiat. Meas.* 41 (2006) 649–658.
- [32] X.L. Wang, A.G. Wintle, Y.C. Lu, Testing a single-aliquot protocol for recuperated OSL dating, *Radiat. Meas.* 42 (2007) 380–391.
- [33] A.G. Wintle, Fifty years of luminescence dating, *Archaeometry* 50 (2008) 276–312.
- [34] A.G. Wintle, A.S. Murray, A review of quartz optically stimulated luminescence characteristics and their relevance in single aliquot regeneration dating protocols, *Radiat. Meas.* 41 (2006) 369–391.